ELSEVIER

Geotextiles and Geomembranes 20 (2002) 213–239

Geotextiles and Geomembranes

www.elsevier.com/locate/geotexmem

Numerical study of the factors affecting the consolidation of clay with vertical drains

Bipul C. Hawlader[a,*], Goro Imai[b], Balasingam Muhunthan[c]

[a] *C-CORE, Morissey Road, St. John's, Newfoundland, Canada A1B 3X5*

[b] *Department of Civil Engineering, Yokohama National University, 79-5 Tokiwadai, Hodogaya-ku, Yokohama 240-8501, Japan*

[c] *Civil and Environmental Engineering, Washington State University, Pullman, WA 99164-2910, USA*

Received 12 January 2002; received in revised form 7 May 2002; accepted 15 May 2002

Abstract

A methodology has been developed for the consolidation analysis of a unit cell of clay around a single vertical drain. An elasto-viscoplastic constitutive model has been used to capture the time dependent consolidation behaviour of clay. The model considers a void ratio rate dependent yield stress to separate pre- and post-yield consolidation processes. The governing equation of the consolidation of clays with vertical drains has been solved using a robust finite difference scheme. A parametric study has been conducted to identify the influence of viscosity and smear on the consolidation process. It has been shown that viscosity has minimal influence on the consolidation process for closely spaced drains whereas its effects are significant for largely spaced drains. The inner smear zone surrounding the drains was found to be the dominant factor in controlling the overall progress of consolidation. Even small sizes of the smear zone significantly can retard the progress of consolidation. The permeability within the inner smear zone has been found to be more important than its extent. A linear variation of permeability within the inner smear zone using the coefficient of permeability of the undisturbed soil and the remolded soils has been shown to capture the important effects of smear on consolidation.

Keywords: Vertical drain; Consolidation; Viscosity; Smear zone; Permeability

*Corresponding author. Tel.: +1-709-737-4312; fax: +1-709-737-4706.

E-mail addresses: bipul.hawlader@c-core.ca (B.C. Hawlader), imaigo@cvg.ynu.ac.jp (G. Imai), muhuntha@wsu.edu (B. Muhunthan).

0266-1144/02/$ - see front matter
PII: S0266-1144(02)00012-2

Nomenclature

σ'	effective stress
C_α	secondary compression index
C_c	compression index
C_s	swelling index
c_r	coefficient of radial consolidation
c_z	coefficient of vertical consolidation
EOP	end of primary consolidation
d_r	distance from the drainage face
e	current void ratio
e_0	initial void ratio
$\dot{e}$	void ratio rate ($\Delta e/\Delta t$)
Δe^{ir}	irrecoverable (plastic + viscous) void ratio change
Δe^{r}	recoverable (elastic) void ratio change
H	height of clay cylinder
k_{r0}	coefficient of radial permeability in undisturbed zone
k_s	coefficient of radial permeability in smear zone
k_z	coefficient of vertical permeability
σ	applied stress at top surface (subscript 'in' for initial and 'f' for final)
r	radial coordinate
r_e	radius of equivalent clay cylinder
r_o	radius of outer smear zone
r_s	radius of inner smear zone
r_w	radius of drain
t	time
Δt	time increment
u	excess pore water pressure
$\bar{U}$	average degree of consolidation
$\bar{U}_r$	degree of consolidation due to radial drainage
$\bar{U}_z$	degree of consolidation due to vertical drainage
z	vertical position in reduced coordinate system
ξ	vertical position in spatial co-ordinate system

1. Introduction

Since the classical solution presented by Barron (1948), a number of researchers (e.g. Raymond, 1969; Yoshikuni and Nakanodo, 1974; Hansbo, 1981; Onoue, 1988; Zeng and Xie, 1989; Hird and Russell, 1992) have investigated the factors affecting the progress of consolidation with vertical drains. The influence of smear on consolidation and the discharge capacity of the drain have been the main focus of such investigations. The term smear is generally referred to the disturbance that occurs during the installation of the vertical drain. Substantial reduction in soil

permeability occurs around the drain as a result of its installation. Most analyses of the consolidation of clays with drains, however, use the coefficient of consolidation as an input parameter. Since the coefficient of consolidation is a combined form of permeability and compressibility, these analyses cannot explicitly account for the effects of permeability. It has been suggested that the use of permeability and compressibility as independent input parameters is a better choice for numerical analysis of the consolidation process (Tavenas et al., 1983). The efficiency of vertical drains on consolidation has also been studied by finite element analysis (Hird and Russell, 1992; Bergado et al., 1993; Chai and Mura, 1999; Zhu and Yin, 2000). Li and Rowe (2001) have examined the combined effect of vertical drains and geosynthetic reinforcement on the performance of embankments on soft clays.

The diameter of the smear zone and its permeability are difficult to be determined from laboratory tests, and so far, there is no effective method to measure them. The extent and permeability of the smear zone has been found to vary with the installation procedure, size and shape of the mandrel, and soil microfabrics. Field and laboratory observations (Onoue et al., 1991; Madhav et al., 1993; Bergado et al., 1996; Indraratna and Redana, 1998) have shown a continuous variation of soil permeability with radial distance away from the centre of the drain. Such permeability variation can be separated into three distinct zones (Onoue et al., 1991; Madhav et al., 1993; Bergado et al., 1996); (i) an inner smear zone near the drain, where permeability is greatly reduced due to the remolding of soil, (ii) an outer smear zone, where soil permeability is reduced slightly as a result of the initial reduction of void ratio during the installation of drain, and (iii) an undisturbed zone, where soil permeability is unaffected by the drain installation.

The diameter of the smear zone has been a subject of intense discussion in the literature. For design purposes, several researchers (e.g. Jamiolkowski and Lancellotta, 1981; Bergado et al., 1996; Hansbo, 1987, 1997; Akagi, 1979) have recommended the use of $(2-3)d_m$, where d_m is the diameter of the circle with an area equal to the cross section of the mandrel. On the other hand, McDonald (1985), Aboshi and Inoue (1986) have recommended the area of the smear zone to be the same as that of the area of the mandrel.

For analysis purposes a constant permeability, which is less than the permeability of the undisturbed soil, is usually adopted for the smear zone. For example, Hansbo (1997) recommended that the coefficient of radial permeability in the smear zone (k_s) as being equal to the coefficient of vertical permeability (k_z) in the undisturbed zone. Based on field and laboratory measurements, however, a ratio of $k_s/k_{r0} = 10$, where k_{r0} is the radial permeability of the undisturbed soil, was found to be appropriate for Bangkok clay (Bergado et al., 1996). Tests performed on the soil specimens collected from field located at different distances from the vertical drain have shown that the permeability of the soil near the drain is reduced to about one fifth of the permeability of the undisturbed soil (Madhav et al., 1993).

Use of constant but different values of permeability for the smear zone and the undisturbed soil is useful to obtain closed form solutions for consolidation with vertical drains. However, the use of two distinct permeability values in the smear and undisturbed regions causes problems during numerical analysis due to the

discontinuity at the interface. Additional assumptions are needed for the nodes at the interface for completing the numerical analysis (Madhav et al., 1993). It is shown later that the use of a continuous variation of permeability within this smear zone is a more appropriate choice and avoids the problems of discontinuity during numerical analysis.

Viscous phenomena in soils are well known but ignored in most of the analyses of clay consolidation with vertical drains (Pilot, 1981). Bergado et al. (1993) have conducted an extensive program of settlement monitoring on a test embankment built on soft Bangkok clay with prefabricated vertical drains. Large-scale laboratory consolidation tests were also performed using the same type of vertical drains installed in the clay sample. Their results summarized in Fig. 1 show that whereas the field and laboratory settlements continued to increase with time, all of the predicted curves become flatter in the end because they did not consider the time effects. In order to model realistically the consolidation of clays with vertical drains, Hansbo (1997) has recommended considering the effects of time during the period of primary consolidation in the analysis. While the mechanism of the origin of time effects in soils remains an intensive subject of research (Murakami, 1988), structural viscosity acting within the soil skeleton is generally assumed to be its primary cause.

In order to take into account of viscosity during primary consolidation constitutive models have been developed as a function of time (e.g. Yin and Graham, 1989; Murakami, 1988) or as a function of strain rate ($\dot{\varepsilon}$) (e.g. Kabbaj et al., 1986). It is therefore necessary to implement these types model into the analysis of consolidation of clays with vertical drains in order to examine the effect of viscosity. It is noted here that some early investigations into the effect of strain rate on consolidation have shown it to be small (e.g. Gibson and Lo, 1961; Smith and Wahls, 1969). Leroueil and Marques (1996) attributed this to the result of the

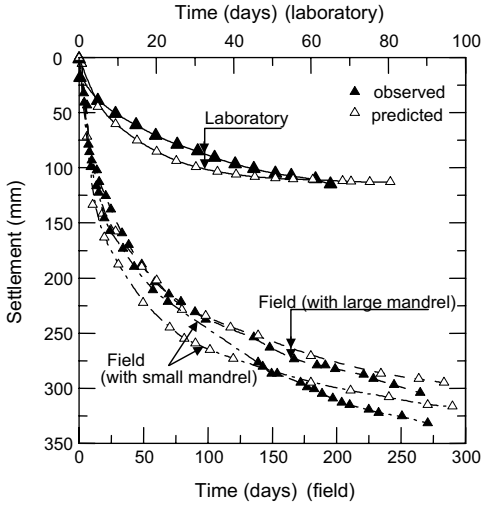

Fig. 1. Time settlement relationships (after Bergado et al., 1993).

structuration of those clays. As shown later, however, the consolidation behaviour of the soil described in this study is dependent upon strain rate.

In this study a numerical algorithm has been developed to solve the governing equation of the one-dimensional consolidation process with vertical drain incorporating a new constitutive model for the clay. The model considers the effect of viscosity during primary consolidation. It has been used previously by the authors (Hawlader et al., 2002) to account for the important effects of viscosity on consolidation in the field. The effects of viscosity on the consolidation process of clays with vertical drains are investigated here. The effect of smear zone is examined in terms of its permeability and its lateral extent.

2. Equivalent clay cylinder with vertical drain

The consolidation process of clay with vertical drains can be idealized with a unit cell model as shown in Fig. 2. The unit cell consists of a soil mass of radius r_e centred with a cylindrical drain of radius r_w. The clay layer rests on a porous bed that is restricted from vertical movement whereas the pervious surface at the top of the clay layer on which load is applied, settles only vertically downward with the progress of consolidation. The discharge capacity of a modern prefabricated vertical drain is considered to be high enough for neglecting the effect of well resistance (Hansbo, 1997).

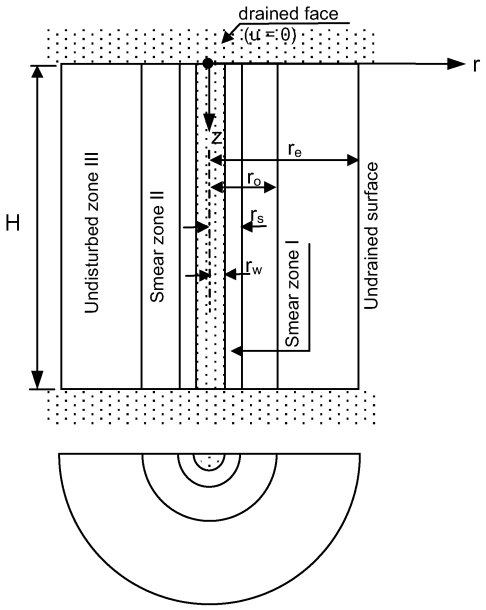

Fig. 2. Schematic view of unit cell for numerical analysis.

3. Consolidation of clay with drainage distance

Imai (1995) developed an interconnected consolidometer to examine the consolidation behaviour (e and σ') of clay elements located at different drainage distances. This device consists of seven sub-cells of 60 mm inside diameter and 5 mm height as shown schematically in Fig. 3(a). Drainage was provided only at the top of the cell arrangement. The sub-specimens were connected to enable a continuous flow of pore water. Additional details of the test and the method of sample preparation have been provided by Imai (1995).

When a consolidation pressure σ is applied at the top of the consolidometer each sub-specimen begins to consolidate. The displacement (d_i) and pore water pressure

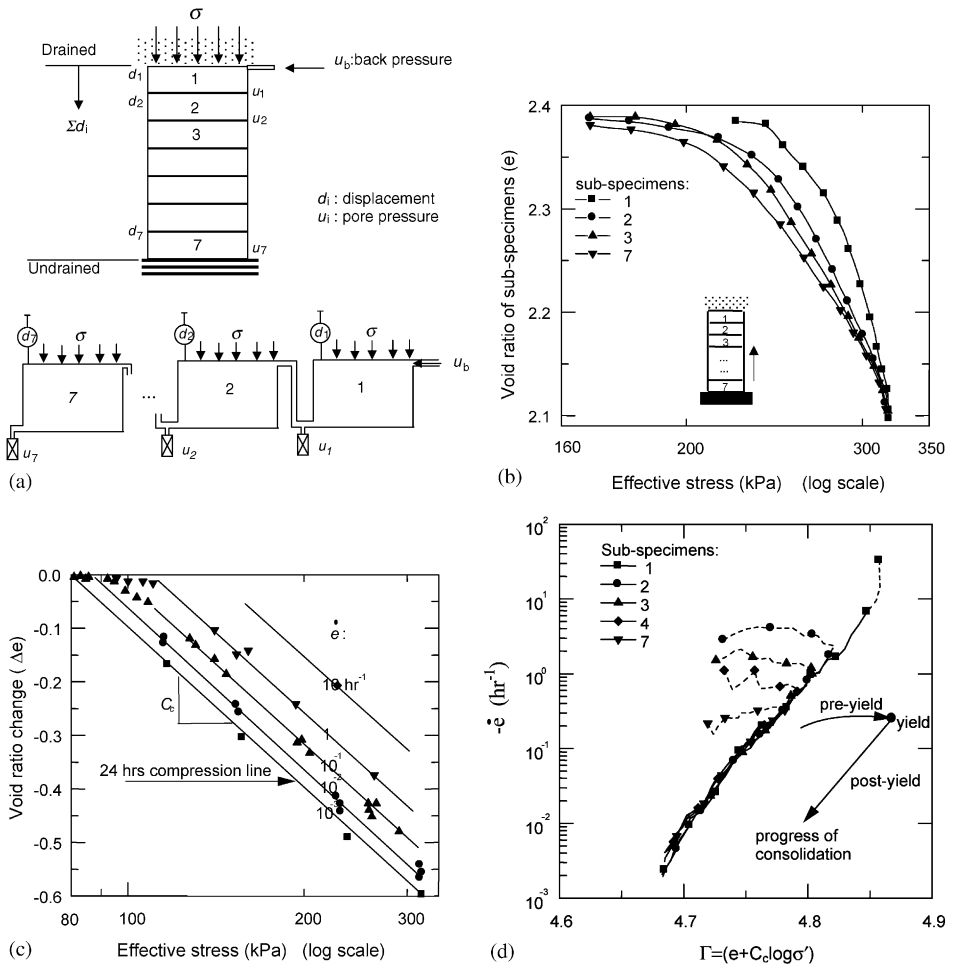

Fig. 3. (a) Basic concept of interconnected consolidation test. (b) State path of sub-specimes. (c) Void ratio rate lines. (d) Relationship between Γ and $\dot{e}$.

(u_i) with time for each sub-specimen is measured. These measurements are used to calculate the changes in effective stress (σ') and void ratio (e) for the total specimen and sub-specimens.

Using this device a series of consolidation tests were performed on reconstituted soil samples prepared from Yokohama Bay Mud. The preconsolidation pressure of all the samples was 49 kPa. The void ratio change for a typical load increment within each sub-cell is shown in Fig. 3(b). This figure shows that the state path ($e - \log \sigma'$) for each sub-specimen during consolidation is different and is dependent on the distance from the drainage face. It is also seen that the changes in void ratio with effective stress is small during the initial stages for all sub-elements followed by a rapid reduction after some stress clearly evidencing yield type behaviour. The term 'yield' is used to separate small and large strains during the progress of consolidation (Leroueil, 1997). Note that this yield stress is a rheological phenomenon that results from the time effect under previous stress state on a normally consolidated soil (Murakami, 1988; Imai, 1995). It is different from the conventional preconsolidation pressure that results from the unloading of the soil element (Leroueil, 1997).

The void ratio rate ($-\dot{e} = \Delta e/\Delta t$) during consolidation for different load increment ratios (LIRs) (78.4 → 235.2 kPa; 78.4 → 313.6 kPa; 156.8 → 313.6 kPa; 235.2 → 470.4 kPa) is shown in Fig. 3(c). It can be seen that despite the different LIRs used, the void ratio rate lines lie parallel to each other. The slope of the parallel lines was found to be approximately equal to the compression index C_c in an $e - \log \sigma'$ plot (Imai, 1995).

The void ratio rate is plotted against the specific parameter Γ ($= e + C_c \log \sigma'$, Hawley and Borin, 1973; where σ' is in kPa) in Fig. 3(d). Γ is a parameter that defines the relative position of the current state of the soil element (e, σ') measured from the basic compression line which passes through the initial state point (e_0, σ'_0) (point A in Fig. 4(b)) and having the slope C_c (Hawley and Borin, 1973). The solid lines in Fig. 3(d) denote the post-yield changes in void ratio rate of the sub-specimens with Γ. A unique linear relation can represent these changes in void ratio rate with Γ of all the sub-specimens irrespective of their location:

$$\Gamma = a \log(-\dot{e}) + b, \tag{1}$$

a and b are soil constants whose values can be obtained from a one-dimensional consolidation test (Imai, 1995). The constant a has been found to be related to the structural viscosity of the clay skeleton. In fact, experimental results have shown that a is approximately equal to the coefficient of secondary compression, C_α (Imai and Tang, 1992; Imai, 1995).

Imai (1995) also found that if the total void ratio change is separated into its recoverable (Δe^r) and irrecoverable (Δe^{ir}) components then the latter (Δe^{ir}) can also be represented by a relation similar to Eq. (1).

$$e^{ir} + C_c \log \sigma' = C_\alpha \log(-\dot{e}^{ir}) + b. \tag{2}$$

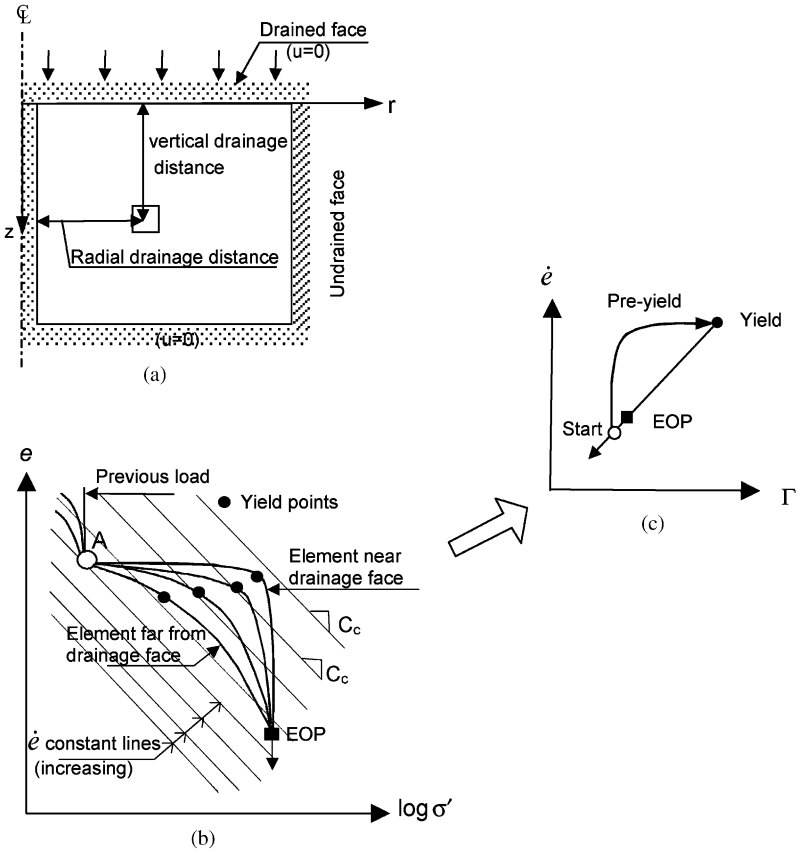

Fig. 4. Proposed consolidation model.

4. Proposed consolidation model

The above observations on the distinct consolidation behaviour of elements with respect to their distance from the drainage face has been used to formulate a constitutive model for the consolidation analysis of clays with vertical drains. The underlying ideas of the proposed model are shown schematically in Fig. 4(b). In this figure, the inclined parallel lines are the void ratio rate ($-\dot{e}$) lines and represent the time effects on consolidation. Suppose a clay specimen begins to consolidate from an initial state A (Fig. 4(b)). If the applied stress is larger than yield stress, the specimen will first experience void ratio changes due to the initial non-linear elastic deformation followed by post-yield deformation governed by Eq. (1). In order to determine the state of yield, we form (see Eq. (1)):

$$\Delta f = [e + C_c \log \sigma'] - [C_\alpha \log(-\dot{e}) + b]. \tag{3}$$

The value of Δf is calculated for each step by using the current values (e, σ', $\dot{e}$). The first [ ] term on the right-hand side of Eq. (3) is the current value of Γ before yield and the second [ ] term is the expected value of Γ if the soil element is in complete yield against the current value of $\dot{e}$. The magnitude of Δf is then a measure of the closeness of the state of a soil element that is to yield. Its value is zero when an element yields.

Note that the rate of compression for each element within the clay layer is different, since compression is associated with the expulsion of pore water and viscosity. The pore water pressure dissipation depends on the drainage distances (z, r) (see Fig. 4(a)). Therefore, for elements near the drainage boundary effective stresses will increase rapidly. As a result, their compression curves will experience higher void ratio rates. For elements away from the drainage boundaries, however, pore pressures will dissipate slowly. Consequently, these elements will have a delayed compression before reaching the same level of effective stress as an element near the drainage faces. As a result, elements at larger distances from the drainage boundaries will follow further down in the system of parallel ($-\dot{e}$) lines than those elements at a shorter distances from drainage boundary in an effective stress–void ratio plot. Notice that the points of yield denoted by solid circles (Fig. 4(b)) are also dependent on the drainage distance. Yield stress will be higher for elements near the drainage boundaries.

5. Void ratio changes

The total change in void ratio (Δe) of a consolidating soil element is separated into two components; recoverable (Δe^{r}) and irrecoverable (Δe^{ir}). The recoverable component associated with any increment of stress is defined by

$$-\Delta e^{\mathrm{r}} = C_{\mathrm{s}}\Delta \log \sigma' = 0.434\, C_{\mathrm{s}}\frac{\Delta\sigma'}{\sigma'}, \tag{4}$$

where C_{s} is the swelling index. Since the initial portion of the void ratio curve is non-linear elastic and dependent on viscosity, the change in void ratio prior to yield is calculated by a slightly modified form of Eq. (4):

$$-\Delta e = 0.434 C_{\mathrm{t}}\Delta\sigma'/\sigma', \tag{5}$$

where, $C_{\mathrm{t}} = C_{\mathrm{s}} + (C_{\mathrm{c}} - C_{\mathrm{s}})/(1 + \mu\Delta f)$. Based on the best-fit curve of the test results for the pre-yield consolidation process, a value of $\mu = 100$ is used in this study. The use of C_{t} enables a gradual change in compressibility from pre-yield to post-yield consolidation conditions.

The irrecoverable component, (Δe^{ir}), occurs after yielding and consists of plastic and viscous parts. Since $\dot{e}^{\mathrm{ir}}$ is a function of σ' and e^{ir} (Eq. (2)), using chain rule:

$$\Delta(-\dot{e}^{\mathrm{ir}}) = f_{\sigma'}\Delta\sigma' + f_{e^{\mathrm{ir}}}\Delta e^{\mathrm{ir}}, \tag{6}$$

where

$$f_{e^{ir}} = \frac{-\dot{e}^{ir}}{0.434C_\alpha}, \quad f_{\sigma'} = \frac{C_c}{C_\alpha}\frac{-\dot{e}^{ir}}{\sigma'}.$$

The average void ratio rate ($-\dot{e}^{ir}_{av}$) between time t and $t+\Delta t$ is:

$$-\dot{e}^{ir}_{av} = (-\dot{e}^{ir}) + \Delta(-\dot{e}^{ir})/2. \tag{7}$$

Combining Eqs. (6) and (7) and making use of $\Delta e^{ir} = \dot{e}^{ir}_{av}\Delta t$, a relationship among Δe^{ir}, $\Delta\sigma'$ and Δt can be established as

$$-\Delta e^{ir} = \frac{f_{\sigma'}\Delta t}{2+f_{e^{ir}}\Delta t}\Delta\sigma' - \frac{2\dot{e}^{ir}\Delta t}{2+f_{e^{ir}}\Delta t}, \tag{8}$$

The total void ratio change Δe during post-yield consolidation is obtained by combining Eqs. (4) and (8):

$$-\Delta e = -(\Delta e^{r} + \Delta e^{ir}) = A_1\Delta\sigma' + B_1\Delta t, \tag{9}$$

where

$$A_1 = 0.434\frac{C_s}{\sigma'} + \frac{f_{\sigma'}\Delta t}{2+f_{e^{ir}}\Delta t},$$

and

$$B_1 = \frac{-2\dot{e}^{ir}}{2+f_{e^{ir}}\Delta t}.$$

Note that the Eq. (9) can be used for pre-yield consolidation with $A_1 = 0.434C_t/\sigma'$ and $B_1 = 0$ (Eq. (5)).

6. Governing equations

The law of conservation of mass for the combined effects of radial and vertical drainage of water from a soil element is (Appendix A):

$$\frac{\partial e}{\partial t} = (1+e)\left(\frac{\partial v_r}{\partial r} + \frac{v_r}{r}\right) + \frac{\partial v_z}{\partial z}, \tag{10}$$

where

$$v_r = \frac{k_r}{\gamma_w}\left(\frac{\partial u}{\partial r}\right)$$

is the radial seepage velocity and

$$v_z = \frac{k_z}{\gamma_w}\left(\frac{1}{1+e}\frac{\partial u}{\partial z} - \gamma_w\right)$$

is the vertical seepage velocity. k_z and k_r are the coefficients of permeability in vertical and radial direction respectively.

The coefficient of permeability in the vertical direction (k_z) is assumed to vary with void ratio as (Tavenas et al., 1983; Imai and Tang, 1992)

$$\log k_z = \log k_{z0} - \frac{e_0 - e}{C_k}, \tag{11}$$

where k_{z0} is the coefficient of vertical permeability at initial void ratio (e_0) and C_k is the permeability change index ($\approx 0.5e_0$,Tavenas et al., 1983).

The coefficient of permeability in the radial direction (k_r) is related to the coefficient of permeability in the vertical direction (k_z) by a ratio R (Rixner et al., 1986; Tavenas et al., 1983):

$$\frac{k_r}{k_z} = R. \tag{12}$$

The magnitude of R is dependent on the microfabric of soil and depositional environment (Rixner et al., 1986; Tavenas et al., 1983).

Substitution of the expressions of v_r and v_z into Eq. (10) and rearrangement leads to the following compact form of the governing equation of consolidation:

$$\frac{\partial e}{\partial t} = F, \tag{13}$$

where

$$F = \underbrace{\left(C_1\frac{\partial^2 u}{\partial r^2} + C_2\frac{\partial u}{\partial r}\right)}_{\text{radial}} + \underbrace{\left(C_3\frac{\partial^2 u}{\partial z^2} + C_4\frac{\partial u}{\partial z} + C_5\right)}_{\text{vertical}}.$$

The expressions for the coefficients C_i ($i = 1$–5) are provided in Appendix B (Eqs. (B.1)–(B.5)).

Since the change in void ratio (Δe) is related to the change in effective stress through the constitutive equations (Eq. (9)), the term on the left-hand side of Eq. (13) can be expressed as a function of $\Delta\sigma'$. Further, since $\Delta\sigma' = -\Delta u$ during consolidation, Eq. (13) can in turn be expressed in terms of Δu as

$$-\Delta u = [(F - B_1)/A_1]\Delta t. \tag{14}$$

7. Numerical implementation

The governing equation (Eq. (14)) for the problem of consolidation of clays with vertical drains has been solved for values of u using a finite difference scheme. The space-time grid used for this purpose is shown in Fig. 5(a). In this figure, the vertical position of the clay layer in the reduced co-ordinate system (z) is described by suffix 'n' while suffix 'l' is used to denote the radial distance (r) from the centre of the drain. Time constitutes the third dimension of the grid and is denoted by the superscript 'k'.

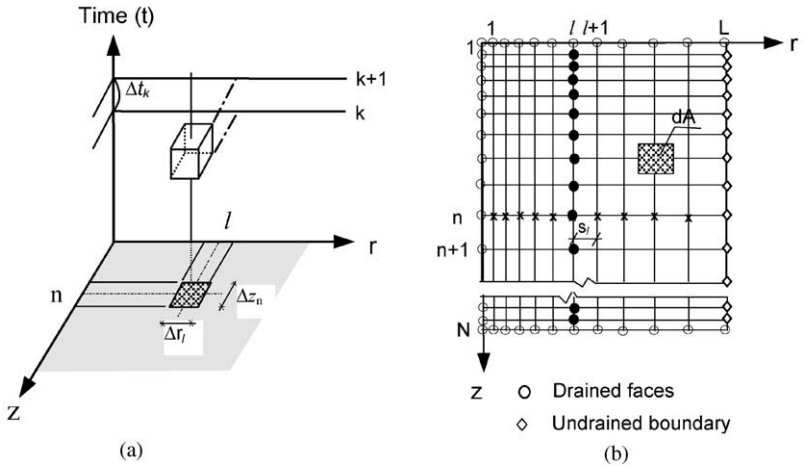

Fig. 5. Finite difference grids in space time domain.

For a grid point (n, l) at the time step k, the finite difference form of Eq. (14) becomes:

$$u^{k+1} = u^k + \left[\left(C_6\frac{\partial^2 u}{\partial r^2} + C_7\frac{\partial u}{\partial r}\right) + \left(C_8\frac{\partial^2 u}{\partial z^2} + C_9\frac{\partial u}{\partial z} + C_{10}\right)\right]\Delta t, \tag{15}$$

where the coefficients, C_i, $i = 6-10$ are related to C_i, $i = 1$–5 through the parameters A_1 and B_1 as shown in Appendix B (Eq. (B.6)). The partial derivatives in Eq. (15) can be expanded using the central difference formulation resulting in

$$\begin{aligned} u_{n,l}^{k+1} = {} & u_{n,l}^k + \{\bar{C}_6(u_{n,l+1}^k - 2u_{n,l}^k + u_{n,l-1}^k) + \bar{C}_7(u_{n,l+1}^k - u_{n,l-1}^k)\}\Delta t \\ & + \{\bar{C}_8(u_{n+1,l}^k - 2u_{n,l}^k + u_{n-1,l}^k) + \bar{C}_9(u_{n+1,l}^k - u_{n-1,l}^k) + \bar{C}_{10}\}\Delta t, \end{aligned} \tag{16}$$

where the coefficients $\bar{C}_i$, $i = 6-10$ are as shown in Appendix B (Eq. (B.7)).

The finite difference equation (Eq. (16)) is solved numerically using the alternating direction implicit (ADI) method (Ganzha and Vorozhtsov, 1996). Use of the ADI scheme provides not only a computationally efficient implicit scheme but also guarantees the stability of the solution (Thomas, 1995).

In order to present the ADI scheme in a compact form, the difference operator of Eq. (16) is rewritten as

$$\Lambda_r(u_{n,l}^k) = \bar{C}_6(u_{n,l+1}^k - 2u_{n,l}^k + u_{n,l-1}^k) + \bar{C}_7(u_{n,l+1}^k - u_{n,l-1}^k), \tag{17}$$

$$\Lambda_z(u_{n,l}^k) = \bar{C}_8(u_{n+1,l}^k - 2u_{n,l}^k + u_{n-1,l}^k) + \bar{C}_9(u_{n+1,l}^k - u_{n-1,l}^k) + \bar{C}_{10}. \tag{18}$$

Accordingly, Eq. (16) can be represented as

$$\frac{u_{n,l}^{k+1} - u_{n,l}^k}{\Delta t} = \Lambda_r(u_{n,l}^k) + \Lambda_z(u_{n,l}^k) \tag{19}$$

and the corresponding ADI scheme is as follows (Mavriplis, 1988):

$$\frac{u_{n,l}^{k+1/2} - u_{n,l}^{k}}{\Delta t/2} = \Lambda_r(u_{n,l}^{k+1/2}) + \Lambda_z(u_{n,l}^{k}), \tag{20}$$

$$\frac{u_{n,l}^{k+1} - u_{n,l}^{k+1/2}}{\Delta t/2} = \Lambda_r(u_{n,l}^{k+1/2}) + \Lambda_z(u_{n,l}^{k+1}), \tag{21}$$

where the superscript $(k + 1/2)$ represents the middle of the time between kth and $(k + 1)$th time steps. For the first half of the time step (Eq. (20)), the radial direction is implicit and vertical direction is explicit while for the second half (Eq. (21)), the radial direction is explicit and vertical direction is implicit in the above scheme.

To facilitate the use of tri-diagonal matrix algorithms (TDMA) for the solution of nodal values, Eqs. (20) and (21) can be rewritten as

$$C_{1r,l}u_{l-1}^{k+1/2} + C_{2r,l}u_{l}^{k+1/2} + C_{3r,l}u_{l+1}^{k+1/2} = C_{4r,l}, \tag{22}$$

$$C_{1z,n}u_{n-1}^{k+1} + C_{2z,n}u_{n}^{k+1} + C_{3z,n}u_{n+1}^{k+1} = C_{4z,n}, \tag{23}$$

where the constants $C_{ir,l}$ and $C_{iz,n}$ are as shown in Appendix B (Eqs. (B.8)–(B.15)).

During the computation, the constants $C_{ir,l}$ $(i = 1, 2, 3, 4)$ in Eq. (22) at the grid points along the radial distance $(l = 2, 3, 4, \ldots, L - 1)$ are calculated for the first half of time step (Fig. 5b). Incorporating the boundary conditions for the nodes 1 and L (i.e., first and last nodes), as described later, the simultaneous equations (Eq. (22)) for the different nodes on the nth layer (marked by crosses on Fig. 5b) are solved to obtain their values of $u^{k+1/2}$. Once the calculation for nth layer is completed, it proceeds to the next $(n + 1)$ horizontal soil layer, and continues until all the grid points of soil mass are covered.

Similarly for the second half of the time step, using Eq. (23), u^{k+1} is calculated at each mesh point at the lth radial distance (denoted by solid circles in Fig. 5b). This calculation also continues until all the grid points of the soil layer are covered. Subsequently, the calculation shifts to the next time step. A complete listing of the computer code that was used in the analyses can be found in Hawlader (1998).

8. Initial and boundary conditions

The solution of the governing differential equation of consolidation requires the use of appropriate initial and boundary conditions. The nature of the drainage at the top and bottom boundaries and along the drain forms the drainage boundary conditions.

8.1. Initial condition

The initial effective stress at a grid point 'n' is (Fig. 5b)

$$\sigma'_{n(0)} = \sigma'_{s(0)} + \gamma'(1 + e)z, \tag{24}$$

where the subscript '0' represents the initial condition. $\sigma'_{s(0)}$ is the initial effective stress at the top surface of the clay layer, $(1+e)z$ is the depth of soil layer, γ' is the submerged unit weight of soil. The initial void ratio at this depth is

$$e_{n(0)} = e_{s(0)} + C_c \log(\sigma'_{n(0)}/\sigma'_{s(0)}). \tag{25}$$

8.2. Drained surfaces

The presence of a fully pervious material within the drain and at the top and bottom surfaces of the clay layer results in the complete dissipation of pore pressure immediately after the application of load. Therefore, the reduction of void ratio of an element at this boundary at some subsequent time will be completely viscous (i.e. $\Delta e = \Delta e^{ir}$ and $\dot{e} = \dot{e}^{ir}$) and is governed by Eq. (2).

For the time steps k and $k+1/2$:

$$\Delta e = \frac{\dot{e}^k + \dot{e}^{k+1/2}}{2}\Delta t/2 = C_\alpha \log\left(\frac{\dot{e}^{k+1/2}}{\dot{e}^k}\right) = 0.434 C_\alpha \frac{\dot{e}^{k+1/2} - \dot{e}^k}{\dot{e}^k} \tag{26}$$

Eq. (24) can be rearranged as

$$\dot{e}^{k+1/2} = \dot{e}^k + \frac{2(\dot{e}^k)^2 \Delta t/2}{0.868 C_\alpha - \dot{e}^k \Delta t/2}. \tag{27}$$

Similarly,

$$\dot{e}^{k+1} = \dot{e}^{k+1/2} + \frac{2(\dot{e}^{k+1/2})^2 \Delta t/2}{0.868 C_\alpha - \dot{e}^{k+1/2} \Delta t/2}. \tag{27a}$$

Once the void ratio rate is known, Δe can be calculated using the following relationships:

$$\Delta e = \frac{\dot{e}^k + \dot{e}^{k+1/2}}{2}\frac{\Delta t}{2} \quad \text{(for time steps } k \text{ to } k+1/2), \tag{28}$$

$$\Delta e = \frac{\dot{e}^{k+1/2} + \dot{e}^{k+1}}{2}\frac{\Delta t}{2} \quad \text{(for time steps } k+1/2 \text{ to } k+1). \tag{28a}$$

8.3. Undrained surface (at $r = r_e$)

Along the undrained periphery of the soil cylinder, pore pressure gradient is always zero, i.e.

$$\left.\frac{\partial u}{\partial r}\right|_{r=r_e} = 0. \tag{29}$$

The finite difference approximation of the above relation leads to

$$u_{n,L} = u_{n,L-1}. \tag{30}$$

9. Analysis

For the problem of consolidation with vertical drains, pore pressure gradients near the drained boundaries are very high, whereas gradients are small for the elements away from it. Therefore, a smaller spacing ($s = 10$ mm) is used at the drainage faces (at $l = 1$, $n = 1$ and $n = N$; Fig. 5b). The radial spacing is increased according to

$$s_{n,l} = s_{n,l-1} + \ln(md_r), \tag{31}$$

where, 'm' is a constant and d_r is drainage distance in mm. The constant m controls the increase in spacing. For this study a value of $m = 0.165$ was used. The spacing in the vertical direction is calculated using a similar equation. The radial and vertical spacing used in the study are shown in Fig. 5(b).

The pore pressure gradients are very high near the drained surfaces immediately after the application of load. Accordingly, the initial time step of the calculation should be kept small enough to achieve an accurate solution. With increase in time pore pressure distribution becomes continuous and flatter, then larger time steps can be used in the calculation (Scott, 1963). Therefore, in the present study, the initial time step (Δt_{in}) of 1 s is used and it is advanced according to the function $\Delta t^k = 1.005 * \Delta t^{k-1}$.

Vertical drains are widely used to increase the stability of clay layers and to reduce the time required for consolidation. Since the overall stability and deformation depend on effective stress or pore pressure of the soil elements, the average degree of consolidation at time t can be considered as a measure of overall improvement of clay layer. It is calculated by

$$\bar{U}(t) = 1 - \frac{\int_A u(z, r, t)\,\mathrm{d}A}{\int_A u_0\,\mathrm{d}A}, \tag{32}$$

where u_0 and u are the initial and current pore water pressures respectively, and $\mathrm{d}A$ is the area of the small element corresponding to a grid point (Fig. 5b).

9.1. Verification of analysis

The soil parameters used in the numerical analyses are listed in Table 1. These parameters are obtained from laboratory tests on Yokohama Bay Mud.

Accuracy of the numerical analysis depends on the proper selection of the space and time grids. In order to validate the grid sizes, first a simple case where pore water flows only in the horizontal direction is considered. The problem is solved using the proposed finite difference technique using $m = 0.165$ (Eq. (31)). The same problem was also solved by Barron's analytical solution. To facilitate the comparison, the horizontal coefficient of consolidation $c_r = 8.3 \times 10^{-9}\,\mathrm{m^2/s}$ ($c_z = k_z\sigma'_z(1 + e)/0.434\gamma_w C_c$ and $c_r = c_z(k_r/k_z)$, Jamiolkowski et al., 1981) was used (see also Table 1) and no effect of viscosity is considered in this particular analysis. The analytical and numerical results match closely as shown in Fig. 6, confirming that the choice of space and time grids is accurate. This grid size is used in the analyses that follow.

Table 1
Parameters used in computation

Parameters	Values
C_s	0.11
C_c	1.05
C_α	0.05
b	5.0
σ_{in}	22 kPa
r_w	50 mm
H	5 m
R	3
C_k	1.2
e_0	2.5
k_{z0}	5×10^{-10} m/s
μ	100
σ_f	55 kPa
r_e	600 mm
m	0.165

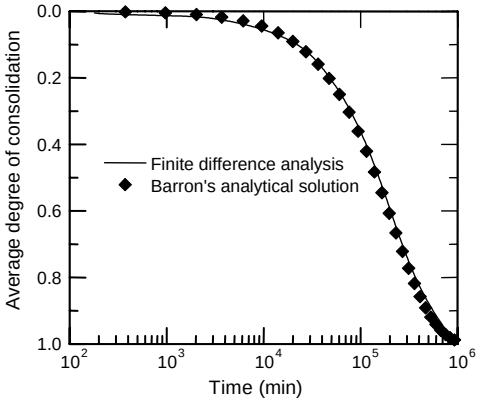

Fig. 6. Accuracy of finite difference solution.

9.2. Comparison with analytical models

The overall degree of consolidation ($\bar{U}$) of a clay layer with vertical drains is the result of the combined effect of radial and vertical drainage. The combined degree of consolidation due to radial drainage ($\bar{U}_r$) and vertical drainage ($\bar{U}_z$) can be calculated using Barron's and Terzaghi's analytical solution respectively. Carillo (1942) combined these two effects as

$$\bar{U} = 1 - (1 - \bar{U}_z)(1 - \bar{U}_r). \tag{33}$$

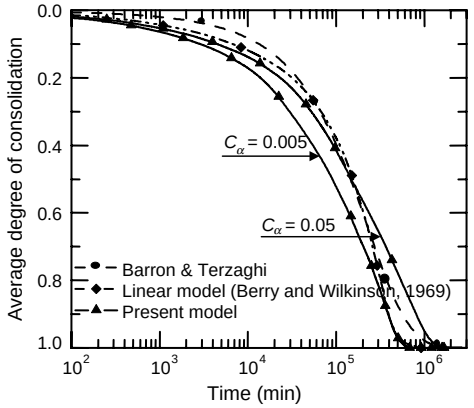

Fig. 7. Comparison between present and available solutions.

The average degree of consolidation $\bar{U}$ with time obtained from the current numerical analysis (Eq. (32)) is shown in Fig. 7 for two different values of C_α. C_α reflects the effect of viscosity (Eq. (1)). Fig. 7 also shows the result for $\bar{U}$ obtained using the analytical solution by Carrillo (Eq. (33)) as well as that obtained using a linear consolidation model (Berry and Wilkinson, 1969) without viscosity (i.e. $\Delta e = C_c \Delta \log \sigma'$). Note that the coefficients of consolidation (c_r and c_z) for the analytical solution calculated in the same manner as described before. It can be seen that the overall degree of consolidation obtained from the present numerical model is higher initially than the other two models. This is as a result of the lower compressibility (i.e. higher coefficients of consolidation) during the pre-yielding consolidation process. Once a soil element begin to yield the compressibility increases and the progress of consolidation slows down. Therefore, with time the present numerical solution crosses over the analytical solution. It is also seen that higher viscous effect (larger C_α) causes the consolidation to be slower. Paute (1973) has reported similar consolidation behaviour from laboratory tests. He also showed that during the initial stages of the consolidation the pore pressure dissipation is higher and thereby the degree of consolidation in laboratory test is faster than that obtained from analytical solution (Barron, 1948).

9.3. Parametric study

As highlighted in the introduction, several factors control the consolidation process of clays with vertical drains. Among them, the effects of viscosity, the variation of permeability within the smear zone and its extent are crucial to the geotechnical design. Unfortunately, these factors are difficult to be quantified in the field (Hird and Moseley, 2000). Therefore, a parametric study from the numerical analysis is performed to gain some insight into the effects of these factors towards the development of better designs.

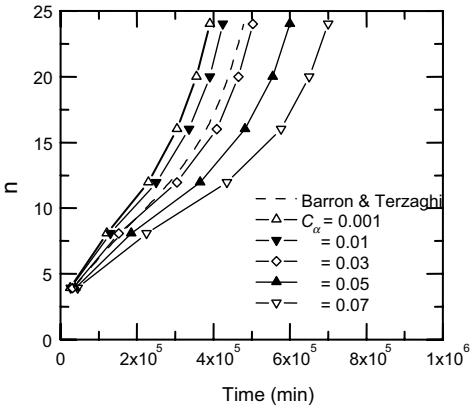

Fig. 8. Effect of viscosity on overall degree of consolidation.

9.3.1. Effect of viscosity related to drain spacing

Fig. 8 shows the time required for 70% overall degree of consolidation with changes in drainage spacing n ($= r_e/r_w$, Fig. 2) and values of C_α. The time required for the same degree of consolidation calculated from the analytical solution (Eq. (33)) is also plotted on this figure. It can be seen that for small n values, the different C_α values have only a small effect on the required time for 70% consolidation. This implies that viscosity effects are not important in the case of closely spaced drains. On the other hand, for large n values C_α has a significant effect on the time for consolidation. Therefore, in the case of large n values, as is the case with modern prefabricated band drains, viscous effects should be taken into account in the calculation of the time for consolidation.

9.3.2. Permeability of the smear zone: non-linear variation

The smear effects caused by the installation of the drains in the clay play a significant role in the consolidation process of clays with vertical drains. These effects have not been taken into account in our analyses reported thus far. Permeability is the key parameter that is affected in the smear zone and its accurate determination is essential for the successful prediction of the consolidation process. In order to examine the influence of the extent and variation of permeability within the smear zone first the non-linear variation of permeability proposed by Onoue et al. (1991) is considered in the analysis. These variations of permeability were obtained form the laboratory test results. According to this model, the permeability within the inner smear zone (see Fig. 2) is defined as

$$k_s = (k_{r0}/\eta_{max})(r/r_o)^{\alpha}(r/r_w)^{\beta} \tag{34}$$

and the permeability of the outer smear zone was defined as

$$k_s = k_{r0}(r/r_o)^{\alpha}, \tag{35}$$

where k_s is the radial permeability in smear zone at a distance r from the centre of the drain. k_{r0} is the radial permeability of the undisturbed soil. r_w and r_o are the radius of

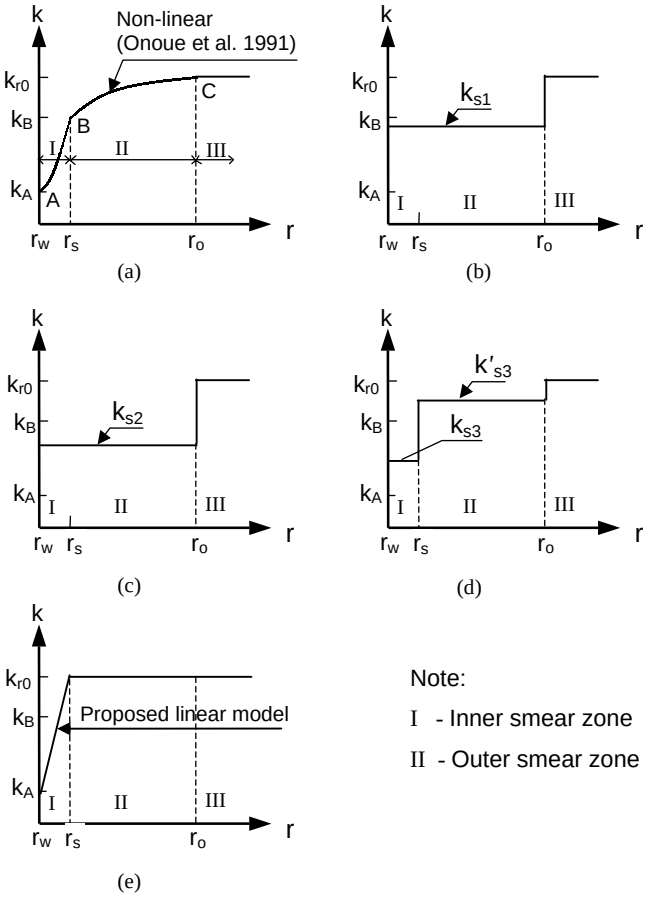

Fig. 9. Radial variation of permeability.

drain and outer smear zone, respectively. α is a function of the void ratio and η_{max} represents the effect of remolding. β is related to α and η_{max} as (Onoue et al., 1991)

$$\beta = \alpha + \log \eta_{max}/\log(r_s/r_w). \tag{36}$$

The permeability variation using the above relationships is shown in Fig. 9(a). The effect of the extent of the inner smear zone (zone-I) on consolidation is examined first by fixing the outer smear zone at a radial distance of $6.5r_w$ (Onoue et al., 1991). Three different sizes of the inner smear zones with $r_s = 1.4r_w$, $1.6r_w$, $3.0r_w$ were considered. Using the variation of the permeability predicted by Eqs. (34) and (35) for each of these inner and outer smear zones, the consolidation problem was solved numerically. The progress of the consolidation with time is shown in Fig. 10(a). It can be seen that consolidation is retarded significantly with an increase in the size of the inner smear zone. This effect is substantial even for a smaller inner smear zone

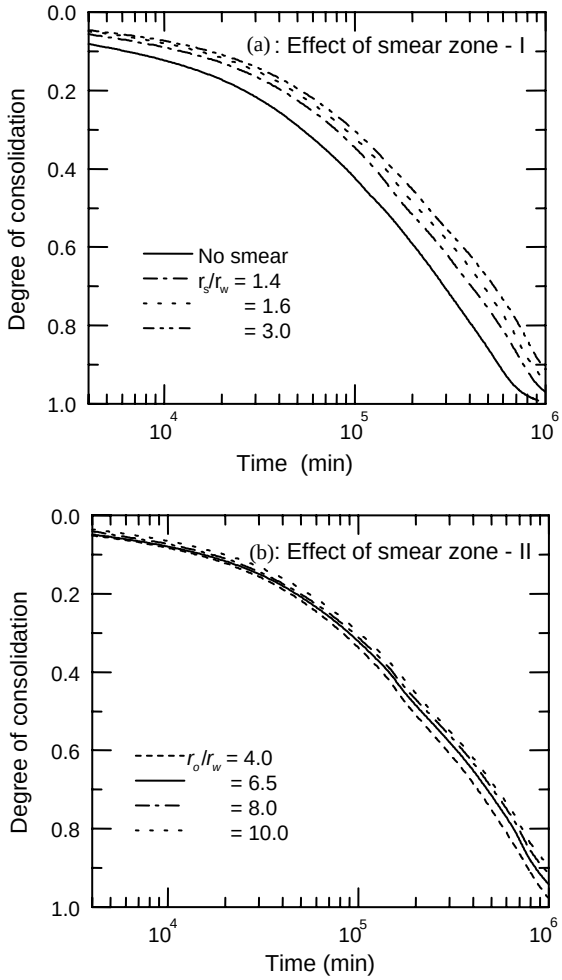

Fig. 10. Influence of extents of smear zones.

with radius $1.4r_w$. The reason behind this is the substantial reduction in the permeability near the drain as a result of the smear.

Analyses were also performed by keeping the inner remolded zone constant at $r_s = 1.6r_w$ and varying the outer zone at $r_o = 3.0r_w$, $6.5r_w$, $8.0r_w$, $10.0r_w$ to examine their influence on consolidation. The results are as shown in Fig. 10(b). Unlike in the case of the inner smear zone (Fig. 10a), the results show that the extent of the outer smear zone does not have much influence on the progress of consolidation.

9.3.3. Permeability of the smear zone: linear variation

In order to examine the feasibility of using a simpler way to account for the variation of permeability within the smear zone, first three different types of

permeability averages are considered: (i) an average value weighted by radial distance (Fig. 9b), $k_{s1} = \sum k_s \Delta r/(r_o - r_w)$ (ii) a simple average (Fig. 9c), $k_{s2} = (k_{r=r_w} + k_{r=r_o})/2$, and (iii) a two step simple average (Fig. 9d), $k_{s3} = (k_{r=r_w} + k_{r=r_s})/2$ and $k'_{s3} = (k_{r=r_s} + k_{r=r_o})/2$. In addition, as shown in Fig. 9(e), the possibility of using a linear variation of permeability within the inner smear zone is considered in the analysis. In the latter case, the permeability at $r = r_w$ is the soil permeability of the remoulded soil (Eq. (34)) while at $r = r_s$ it is the permeability of undisturbed soil.

Bergado et al. (1996) have reported that the smear zone in the field is wider than the result of laboratory tests. Therefore, although $r_s = 1.6r_w$ was measured by Onoue et al. (1991) from laboratory tests a higher radius for the inner smear zone may be required for realistic calculations. On the other hand, Hird and Moseley (2000) have showed that the effects of permeability in smear zone are negligible beyond a radius of about $3r_w$. Accordingly, the radius of the inner smear zone for the current analysis was fixed at $r_s = 3r_w$. The radius of the outer smear zone was kept fixed at $r_o = 6.5r_w$ because, as shown before, it does not have much effect on the progress of consolidation.

The results of the analyses are as shown in Fig. 11. It is evident from this figure that the degree of consolidation predicted using the linear variation of permeability gives a solution very close to that by the non-linear one (Onoue et al., 1991). On the other hand, use of any type of average scheme under estimates the effects of smear. The error will be more with higher reduction of field permeability in the smear zone. These results confirm the observations made previously by Chai et al. (1997) without accounting for viscosity, as is the case here.

Many uncertainties exist regarding the determination of the amount of reduction of permeability within the smear zone. Chai and Mura (1999) have showed that the reduction ratio of k_{r0}/k_s in the field could be as high as 25 times that of k_{r0}/k_s measured in laboratory. In order to examine the effects of permeability reduction,

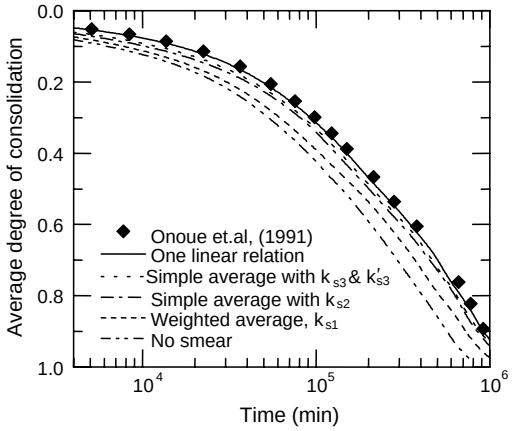

Fig. 11. Effect of permeability variation within smear zone.

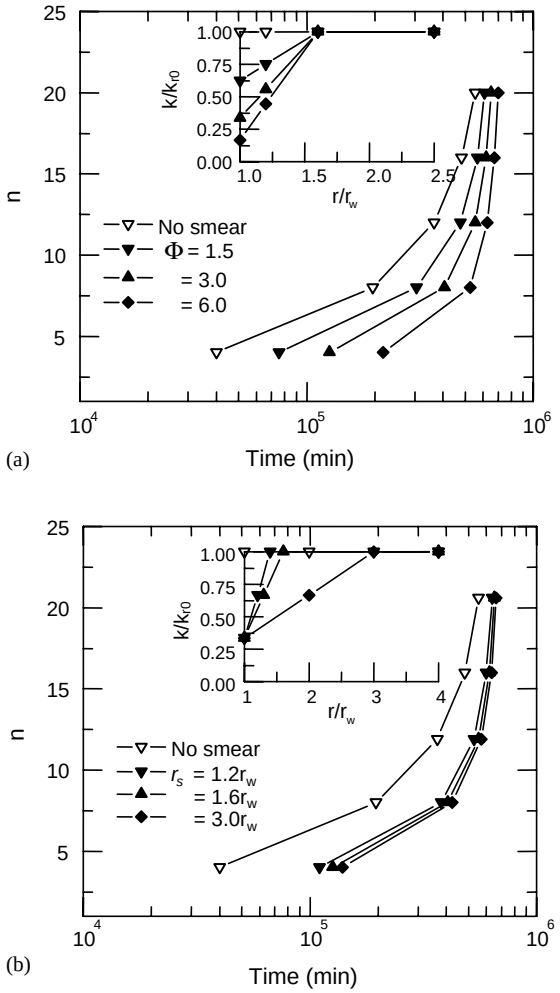

Fig. 12. Effect of extent and permeability of smear zone.

the linear variation of permeability is considered (insets of Fig. 12). The reduction of permeability near the drain is represented by a parameter Φ as

$$\Phi = k_{r0}/k_{s(r=r_w)}. \tag{37}$$

Fig. 12(a) shows the required time for 70% overall degree of consolidation for different value of Φ. It is observed from this figure that Φ has relatively more influence for closely spaced drains. The required time for the same degree of consolidation (70%) for different extents of smear zone with a fixed value of Φ ($=3.0$) is shown in Fig. 12b. Comparison of the results in these figures confirms that

Φ is the dominating factor of consolidation rather than the extent of the smear zone after about $r_s > 2r_w$.

Based on the analyses presented here it appears that once the radius of the smear zone is quantified ($r_s \approx 2r_w$), only two values of coefficient of permeability, namely coefficient of permeability of the undisturbed soil and the remolded soils, are required in order to take into account of the smear effect using the linear variation of permeability in the smear zone. The coefficient of permeability of the undisturbed soil (at $r = r_s$) can be obtained from back-analysis of the case histories or measured in the field using available equipment (Tavenas et al., 1986). The coefficient of permeability near the drain (at $r = r_w$) can be obtained from laboratory tests using the remolded soil (Tavenas et al., 1983).

Finally, it is noted that Barron's solution (1948) are commonly presented in the form of normalized design charts for use by engineers. Unfortunately, inclusion of viscosity effects, yield, and permeability variation with void ratio and radial distance in the scheme presented contains a large number of variables. Therefore, development of normalized design charts is impractical. Instead, it is suggested to use a numerical technique such as the one described here to provide a direct solution to consolidation of clays with vertical drains.

10. Conclusions

A constitutive model that accounts explicitly for the influence of clay structure viscosity and drainage length on the consolidation of clays has been developed. The model considers the void ratio rate dependent yield stresses to separate pre- and post-yield consolidation process. It has been used in the numerical solution of the governing equation of the consolidation of clays with vertical drains. The study uses permeability and compressibility as separate inputs rather than using the coefficient of consolidation. The model was also used to study the effects of smear on the consolidation process.

The numerical solution was verified by comparing the results with analytical solutions. It was then used to perform a parametric study to identify the effects of key variables on the consolidation of clays with vertical drains. Based on this study the following conclusions can be drawn:

(a) The viscosity of clays has only a small influence on the consolidation process for closely spaced drains i.e. lower n-values. Viscosity effects are significant for largely spaced drains.
(b) The overall progress of consolidation is mainly controlled by the inner smear zone surrounding the drains (zone-I). The outer smear (zone-II) has little influence. It has been shown that even small size of the inner smear zone significantly retards the progress of consolidation. The variation of permeability within the inner smear zone is more important than its extent.
(c) Any type of average values of permeability under estimates the effects of smear. A linear variation of permeability within the inner smear zone using the

coefficient of permeability of the undisturbed soil and the remolded soils is able to capture the important effects of smear on consolidation.

Acknowledgements

The work presented in this paper is based on the first authors Ph.D. research at Yokohama National University and collaborative research at Cambridge University. The research in Japan was supported by GRANT-IN-AID FOR SCIENTIFIC RESEARCH (PROJECT NUMBER B-2, 08455219) of the Ministry of Education, Science, Sports and Culture, Japan. This support is gratefully acknowledged. The third author acknowledges the International Fellowship Award by the US National Science Foundation (INT-9802887) that enabled the collaborative effort at Cambridge University with the first author.

Appendix A

With reference to Fig. 13, the vertical and horizontal inflow and outflow of water for a small clay element at radial distance r at time Δt are:

$$\Delta q_{z\_\text{in}} = \left(v_z + \frac{\partial v_z}{\partial \xi}\Delta\xi\right) r\theta\Delta r\Delta t, \tag{A.1}$$

$$\Delta q_{z\_\text{out}} = v_z r\theta\Delta r\Delta t, \tag{A.2}$$

$$\Delta q_{r\_\text{in}} = \left(v_r + \frac{\partial v_r}{\partial r}\Delta r\right)(r + \Delta r)\theta\Delta\xi\Delta t, \tag{A.3}$$

$$\Delta q_{r\_\text{out}} = v_r r\theta\Delta\xi\Delta t. \tag{A.4}$$

Therefore the net volume change is

$$\Delta q = (\Delta q_{r\_\text{in}} - \Delta q_{r\_\text{out}}) + (\Delta q_{z\_\text{in}} - \Delta q_{z\_\text{out}}). \tag{A.5}$$

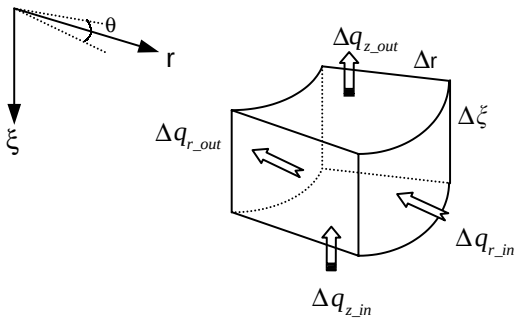

Fig. 13. Water flow of a clay element.

Using Eqs. (A.1)–(A.5), the law of mass conservation for the combined process of vertical and horizontal drainage of water from the soil element can be written as

$$\frac{\partial e}{\partial t} = (1+e)\left(\frac{\partial v_r}{\partial r} + \frac{v_r}{r}\right) + \frac{\partial v_z}{\partial z}, \tag{A.6}$$

where, $\Delta\xi = (1+e)\Delta z$ (Imai, 1995).

Appendix B

$$C_1 = \frac{(1+e)k_r}{\gamma_w}, \tag{B.1}$$

$$C_2 = \frac{1+e}{\gamma_w}\left(\frac{k_r}{r} + \frac{\partial k_r}{\partial r}\right), \tag{B.2}$$

$$C_3 = \frac{1}{\gamma_w}\frac{k_z}{1+e}, \tag{B.3}$$

$$C_4 = \frac{1}{\gamma_w}\left(-\frac{k_z}{(1+e)^2}\frac{\partial e}{\partial z} + \frac{1}{1+e}\frac{\partial k_z}{\partial z}\right), \tag{B.4}$$

$$C_5 = \frac{\partial k_z}{\partial z}, \tag{B.5}$$

$$C_6 = \frac{C_1}{A_1}, \quad C_7 = \frac{C_2}{A_1}, \quad C_8 = \frac{C_3}{A_1}, \quad C_9 = \frac{C_4}{A_1}, \quad C_{10} = \frac{C_5}{A_1} + B_1, \tag{B.6}$$

$$\bar{C}_6 = \frac{4C_6}{(r_{n,l+1} - r_{n,l-1})^2}, \quad \bar{C}_7 = \frac{C_7}{r_{n,l+1} - r_{n,l-1}},$$
$$\bar{C}_8 = \frac{4C_8}{(r_{n+1,l} - r_{n-1,l})^2}, \quad \bar{C}_9 = \frac{C_9}{r_{n+1,l} - r_{n-1,l}}, \quad \bar{C}_{10} = C_{10}, \tag{B.7}$$

$$C_{1r,l} = (-\bar{C}_6 + \bar{C}_7)\Delta t/2, \tag{B.8}$$

$$C_{2r,l} = (1 + 2\bar{C}_6\Delta t/2), \tag{B.9}$$

$$C_{3r,l} = -(\bar{C}_6 + \bar{C}_7)\Delta t/2, \tag{B.10}$$

$$C_{4r,l} = u^k_{n,l} + \{\bar{C}_8(u^k_{n+1,l} - 2u^k_{n,l} + u^k_{n-1,l}) + \bar{C}_9(u^k_{n+1,l} - u^k_{n-1,l}) + \bar{C}_{10}\}\Delta t/2, \tag{B.11}$$

$$C_{1z,n} = (-\bar{C}_8 + \bar{C}_9)\Delta t/2, \tag{B.12}$$

$$C_{2z,n} = (1 + 2\bar{C}_8\Delta t/2), \tag{B.13}$$

$$C_{3z,n} = -(\bar{C}_8 + \bar{C}_9)\Delta t/2, \tag{B.14}$$

$$C_{4z,n} = u_{n,l}^{k+1/2} + \{\bar{C}_6(u_{n,l+1}^{k+1/2} - 2u_{n,l}^{k+1/2} + u_{n,l-1}^{k+1/2}) + \bar{C}_7(u_{n,l+1}^{k+1/2} - u_{n,l-1}^{k+1/2}) + +\bar{C}_{10}\}\Delta t/2. \quad \text{(B.15)}$$

References

Aboshi, H., Inoue, T., 1986. Prediction of consolidation settlement of clay layers, especially in the case of soil stabilization by vertical drain. Proceedings of the IEM-JSSMFE joint Symposium on Geotechnical Problems, Japan, pp. 31–40.

Akagi, T., 1979. Consolidation caused by mandrel-driven sand drains. Proceedings of the Sixth Asian Regional Conference Soil Mechanics and Foundation Engineering, Singapore, Vol. 1, pp. 125–128.

Barron, R.A., 1948. Consolidation of fine-grained soils by drain wells. ASCE Transactions 113 (2346), 718–743.

Bergado, D.T., Mukhergee, K., Alfaro, M.C., Balasubramanium, A.S., 1993. Prediction of vertical-band-drain performance by the finite element method. Geotextiles and Geomembranes 12, 567–586.

Bergado, D.T., Anderson, L.R., Mura, N., Balasubramanium, A.S., 1996. Soft Ground Improvement in Lowland and other Environments. ASCE Press, New York (Chapter 4).

Berry, P.L., Wilkinson, W.B., 1969. The radial consolidation of clay soils. Géotechnique 19 (2), 253–284.

Carillo, N., 1942. Simple two- and three-dimensional cases in the theory of consolidation of soils. Journal of Mathematics and Physics 21 (1), 1–5.

Chai, J.C., Mura, N., 1999. Investigation of factors affecting vertical drain behaviour. ASCE Journal of Geotechnical and Geoenvironmental Engineering 125 (3), 216–226.

Chai, J.C., Mura, N., Sakajo, S., 1997. A theoretical study of smear effect around vertical drain. Proceedings of the 14th ICSMFE, Hamburg, Vol. 3, pp. 1581–1584.

Ganzha, V.G., Vorozhtsov, E.V., 1996. Numerical Solutions for Partial Differential equations: Problem Solving Using Mathematica. CRC press LLC, Boca Raton (Chapter 3).

Gibson, R.E., Lo, K.Y., 1961. A theory of consolidation of soils exhibits secondary compression. Acta Polytechnica Scandinavia, Ci 10, 296.

Hansbo, S., 1981. Consolidation of fine-grained soil by prefabricated drain. Proceedings of the Tenth ICSMFE, Vol. 3, Stockholm, pp. 677–682.

Hansbo, S., 1987. Design aspects of vertical drains and lime column installations. Proceedings of the Ninth Southeast Asian Geotechnical Conference. Bangkok, Thailand, Vol. 2, pp. 8–12.

Hansbo, S., 1997. Practical aspects of vertical drain design. Proceedings of the 14th ICSMFE, Hamburg, Vol. 3, pp. 1749–1752.

Hawlader, B.C., 1998. Elasto-viscoplastic analysis of one-dimensional consolidation of soft clay. Ph.D. Thesis, Engineering Department, Yokohama National University, Japan.

Hawlader, B.C., Muhunthan, B., Imai, G., 2002. Viscosity effects on one-dimensional consolidation of clay. International Journal of Geomechanics, in press.

Hawley, J.G., Borin, D.L., 1973. A unified theory for consolidation of clays. Proceedings of the Eighth ICSMFE, Moscow, Vol. 1.3, pp. 107–119.

Hird, C.C., Moseley, V.J., 2000. Model study of seepage in smear zones around vertical drains in layered soil. Géotechnique 50 (1), 89–97.

Hird, C.C., Russell, D., 1992. Finite element modelling of vertical drains beneath embankments on soft ground. Géotechnique 42 (3), 499–511.

Imai, G., 1995. Analytical examination of the foundation to formulate consolidation phenomena with inherent time dependence. Key Note Lecture, Compression and Consolidation of Clayey Soil, Vol. 2. Balkema, IS-Hiroshima, Japan, pp. 891–935.

Imai, G., Tang, Y.X., 1992. A constitutive equation of one-dimensional consolidation derived from inter-connected tests. Soils and Foundation 32 (2), 83–96.

Indraratna, B., Redana, I.W., 1998. Laboratory determination of smear zone due to vertical drain installation. ASCE Journal of Geotechnical and Geoenvironmental Engineering 124 (2), 180–185.

Jamiolkowski, M., Lancellotta, R., 1981. Consolidation by vertical drain-uncertainties involved in prediction of settlement rates. Panel Discussion, Proceedings of the Tenth ICSMFE, Stockholm, Vol. 4, pp. 593–595.

Kabbaj, M., Oka, F., Leroueil, S., Tavenas, F., 1986. Consolidation of natural clays and laboratory testing. ASTM STP, 892, pp. 378–404.

Leroueil, S., 1997. Critical state soil mechanics and the behaviour of real soils. Symposium on Recent Developments in Soil and Pavement Mechanics. Rio de Janeiro, Brazil, pp. 1–39.

Leroueil, S., Marques M.E.S., 1996. Importance of strain rate and temperature effects in geotechnical engineering. Session on Measuring and Modelling Time Dependent Soil Behaviour. ASCE Convention, Washington, Geotechnique Special Publication, No. 61, pp. 1–60.

Li, A.L., Rowe, R.K., 2001. Combined effects of reinforcement and prefabricated vertical drains on embankment performance. Canadian Geotechnical Journal 38 (6), 1266–1282.

Madhav, R., Park, Y.M., Miura, N., 1993. Modelling and study of smear zones around band shaped drains. Soils and Foundations 33 (4), 135–147.

Mavriplis, D.J., 1988. Multigrid solution of two-dimensional Euler equations on unstructured triangular meshes. American Institute of Aeronautics and Astronautics Journal 26, 824–832.

McDonald, P., 1985. Settlement of fills on soft clay with vertical drains. Proceedings of the 11th ICSMFE, San Francisco, Vol. 8/c/15, pp. 2213–2216.

Murakami, Y., 1988. Secondary compression in the stage of primary consolidation. Technical Note. Soils and Foundations 28 (3), 169–174.

Onoue, A., 1988. Consolidation by vertical drains taking well resistance and smear into consideration. Technical note. Soils and Foundations 28 (4), 165–174.

Onoue, A., Ting, N., Germaine, J.T., Whitman, R.V., Mori, N., 1991. Smear zone around a drain pile and well resistance of drains. Proceedings of the Geo-coast '91. Yokohama, 2/19, pp. 245–250.

Paute, J.L., 1973. Essi oedomètrique à drain central. Bull. Liais. Lab. Ponts Chauss, Special No T.322–334.

Pilot, G., 1981. Method of improving the engineering properties of soft soil. In: Brand, E.W., Brenner, R. P. (Eds.) Soft Clay Engineering. Elsevier, Amsterdam, pp. 637–696.

Raymond, G.P., 1969. Consolidation of deep deposits of homogeneous clays. Géotechnique 19 (4), 478–494.

Rixner, J.J., Kraemer, S.R., Smith, A.D., 1986. Prefabricated vertical drains, Vol. 1: Engineering Guidelines. Report FHWA-RD-86/168, US Federal Highway Administration, Washington DC.

Scott, R.F., 1963. Principles of Soil Mechanics. Addison-Wesley, Reading, MA.

Smith, R.E., Wahls, H.E., 1969. Consolidation under constant rates of strain. Journal of Soil Mechanics and Foundation Engineering Division, ASCE 95 (SM2), 519–539.

Tavenas, F., Jean, P., Leblond, P., Leroueil, S., 1983. The permeability of natural clays, Part II: permeability characteristics. Canadian Geotechnical Journal 20 (4), 645–660.

Tavenas, F., Tremblay, M., Larouche, G., Leroueil, S., 1986. In situ measurement of permeability in soft clays. ASCE Specific Conference on the Use of In Situ Tests in Geotechnical Engineering. ASCE, New York, pp. 1034–1042.

Thomas, J.W., 1995. Numerical Partial Differential Equations: Finite Difference Methods. Springer-Verlag, New York.

Yin, J.H., Graham, J., 1989. Viscous-elastic-plastic modeling of one-dimensional time-dependent behavior of clays. Canadian Geotechnical Journal 26 (2), 199–209.

Yoshikuni, H., Nakanodo, H., 1974. Consolidation of soils by vertical drain wells with finite permeability. Soils and Foundations 14 (2), 35–46.

Zeng, G.X., Xie, K.H., 1989. New development of vertical drain theories. Proceedings of the 12th ICSMFE, Rio de Janeiro, Vol. 2, pp. 1435–1438.

Zhu, G., Yin, J.H., 2000. Finite element consolidation analysis of soils with vertical drain. International Journal of Numerical and Analytical Methods in Geomechanics 24, 337–366.